

The Preparation of Hybrid Material of Cobalt Complex into Mesoporous Silica from the Rice Husk

Pornpan Tana¹, Netchanok Jansawang¹, and Patcharaporn Pimchan^{1,*}

¹Department of chemistry, faculty of Science and Technology, Rajabhat Maha Sarakham University, Maha Sarakham 44000, Thailand

Corresponding author e-mail: *patcharaporn145@gmail.com

Received: 8 November 2019 / Revised: 2 February 2020 / Accepted: 7 April 2020

Abstract

A luminescence hybrid material, Bis(8-hydroxyquinoline)cobalt(II) ($\text{Co}(\text{8hq})_2$), was incorporated into the mesoporous silica. To study the preparation of mesoporous silica from rice husk and the development of fluorescence efficiency. The mesoporous silica was prepared by swelling-shrinking mechanism which used the sodium silicate from rice husk as the precursor. The hybrid materials were prepared by solid-state reaction at room temperature with two different routes; the first one was the hybrid material processes via the in situ formation of cobalt(II)chloride hexahydrate ($\text{CoCl}_2 \cdot 6\text{H}_2\text{O}$) as well as 8hq into the mesoporous silica (MCM) mixed ground ($\text{MCM_Co}(\text{8hq})_2$) and the another one was step by step ground of the mesoporous silica, cobalt(II)chloride hexahydrate and 8hq ($\text{MCMCo}(\text{II})_8\text{hq}$). The hybrid materials were characterized by SEM, XRD, FT-IR, AAS, as well as PL. The FT-IR spectra showed the 8hq characteristic at 820, 786, 784, and 747 cm^{-1} that all of the FT-IR spectra shifted to higher frequencies of free 8hq (815, 778, and 739 cm^{-1}), confirming the coordination between cobalt(II) cation and 8-hydroxyquinoline. The excellent photoluminescence of $\text{MCM_Co}(\text{8hq})_2$ revealed at 484 nm and $\text{MCMCo}(\text{II})_8\text{hq}$ demonstrated blue-shifted peak at 474 nm in this comparison, indicating that the formation of different nanostructures and/or packing of bis (8-hydroxyquinoline)cobalt(II) were formed into the mesoporous silica.

Keywords: Hybrid material, Mesoporous silica, Bis(8-hydroxyquinoline)cobalt(II), Rice husk

1. Introduction

In recent years, the luminescence of metal complexes has attracted significant attention due to the coordination chemistry of inorganic and organic components, electron-transfer substitution of metal or ligand provides an effective means can serve as an efficient approach for the development of electroluminescent materials (Singh et al., 2018; Li & Li, 2009). As a common ligand in metal complexes are widely used aromatic rings such as 8-hydroxyquinoline (8hq), pyridine, and benzoic acid that have conjugate double-bonds as well as stronger absorption than metal ions in the ultraviolet (UV) region (Li & Li, 2009; Świdorski et al., 2018; He et al., 2018). Among these ligands, 8hq has attracted much attention because of a variety of one-dimensional (1D) nanostructures of the metal-8-hydroxyquinoline complexes have been obtained such as nanorods, nanowire, and nanoribbon that nanostructures of the complexes are also tunable electronic and optical properties (Li et al., 2012;

Tsuboi et al., 2012; Behzad et al., 2014; Pimchan et al., 2014).

The metal complexes illustrate potential applications in organic light-emitting devices (OLED) and efficient light-conversion molecular devices. However, their practical application in many fields limited by the low light and thermal stability and poor mechanical strength of metal complexes (He et al., 2018; Pimchan et al., 2014). A wide variety of metal chelates were prepared base-on the nanospace of mesoporous silica, boron nitrite porous, and inter layer as an appropriate host solid that an effective way to solve and protect the metal complexes (He et al., 2018; Pimchan et al., 2014; Sábio et al., 2016). These hybrid materials also have been reported to have many possible applications as photocatalyst and so on (Patriarca et al., 2019; Maučec et al., 2018).

As an emerging host, mesoporous silica has attracted much research because of the possibility of tailoring the pore structure, framework composition, and morphologies over a wide range (Lui et al.,

2015; Sohmiya et al., 2015; Kazuyuki et al., 2011). The porous surface of mesoporous silica could be modified by a swelling-shrinking mechanism with proper organic functional groups and provide accessibility for anchoring other substances. This technique offers the advantages of high control of the hybrid chemical composition at low temperature and large-area processing (Sohmiya et al., 2015; Kazuyuki et al., 2011). Accordingly, host-guest complexes have been synthesized from mesoporous silica for such purposes as sensors, adsorption, and optical applications (Zhao et al., 2017; Kudo et al., 2017; Li et al., 2017). Moreover, the immobilization of luminary on rigid support is a very important way to prepare new solid luminescent materials (Li et al., 2017; Zhang et al., 2018). Recently, the preparation of metal complexes base-on mesoporous silica to improve their performances have attracted increased attention. For example, the aluminum quinolate complex was attached covalently to this functionalized SBA-15 by using coordinating ability of bifunctional precursor (Si-SQ) on the surface of mesoporous material and the observed blue-shift in the emission spectra of the prepared Al(8hq)₃ functionalized material is attributed to the improved molecular interactions of grafted Al(8hq)₃ complexes on the surface and electron withdrawing effect of sulfonamide group that covalently linked to the 8hq in grafted precursor (Si-SQ) (Badiei et al. 2011). The adsorption of [Ru(bpy)₃]²⁺ onto aluminum containing mesoporous silicas was conducted and the photoluminescence of the products was examined as a function of the loaded [Ru(bpy)₃]²⁺ amounts. The result suggests that the pore size and the interactions between [Ru(bpy)₃]²⁺ and the pore surface affects the efficiency; the larger pore size and the weaker interactions between and the pore surface results in the higher self-quenching efficiency (Sohmiya and Ogawa, 2011). Thus, the luminescence properties and stabilities of mesoporous silica-based hybrids can be meticulously designed and tuned.

Solid-state reaction is a facile and feasible method for preparing nanomaterial and has achieved some success in fabricating complex materials (Rahman, 2016). It showed that the promising luminescent properties can be obtained by linking the metal complexes to the mesoporous materials (Ma et al., 2019; Vibulyaseak et al., 2019). Therefore, the synthesis of metal complexes in mesoporous silica via solid-state may be

predominant features such as high color quality, wide-viewing angle, wide operating temperature range, and fast response.

In this paper, we reported the preparation of the cobalt (II) complex of 8-hydroxyquinoline (8hq) into mesoporous silica with different methods. The mesoporous silica was prepared from rice husk which was calcined in air. The cobalt (II) complexes of 8-hydroxyquinoline in mesoporous silica were prepared by solid-state between mesoporous silica and Co (II):8hq. The different methods may enhance the luminescence efficiency of Co(8hq)₂ complex by reducing the concentration quenching and self-absorption. The role of preparation processes may affect the molecular structures and/or packing, as well as optical properties of Co(8hq)₂ complex into the porous space.

Table 1. Color and Photoluminescence band of hybrid materials.

Substances	color	λ_{em} (nm)
Co(8hq) ₂	Dark green	492
MCM_Co(8hq) ₂	Orange green	484
MCMCo(II)_8hq	Light green	474

2. Methodology (Materials and Methods)

2.1 Materials

Rice husk (RH) used in this research were obtained from the rice milling process in Thailand. Cetyltrimethylammonium bromide (C₁₉H₄₂NBr, CTAB) was supplied from Sigma-Aldrich Co., Ltd. Cobalt(II)chloride hexahydrate (CoCl₂·6H₂O) was obtained from CARLO ERBA Reagents S.r.l. 8-hydroxyquinoline (C₉H₇NO, 8hq) was supplied from HiMedia Laboratories., and the reagents were analytical grade and were used without further purification.

2.2 Synthesis

2.2.1 Synthesis mesoporous silica (MCM)

In the beginning, the sodium silicate preparation was synthesized by silicon dioxide (SiO₂) from RH. The raw RH was boiled in 1 M HCl solution for 4 h, washed with distilled water, and then dried at 100 °C for 24 h. The dried RH was calcined in a muffle furnace, which was preheated to 900 °C, for 8 h (Bakar et al., 2016). Then, 100 mL of 2 M NaOH and 5 g of SiO₂ were stirring at 80-100 °C for 3 h. After the reaction period and cooling to room temperature the sodium silicate solution (Na₂Si₃O₇) formed was filtered and stored in a sealed

polypropylene flask at room temperature (Pimprom et al., 2015). Finally, the mesoporous silica was synthesized by the amount 0.8448 g of CTAB, 70.8 mL of deionized water, 800 mL of 99% methanol, and 29.2 mL of 28% aqueous ammonia were mixed and the mixture was stirred for 3 h at 20 °C. The 1.48 mL $\text{Na}_2\text{Si}_3\text{O}_7$ was added to the solution and then the suspensions were aged at 4 °C for another 24 h. The solid particles were collected by evaporation. The product was calcined in air at 660 °C for 10 h to form a porous silica shell. The molar ratio of $\text{MCM}:\text{C}_{18}\text{TAB}:\text{H}_2\text{O}:\text{NH}_3:\text{MeOH}$ was 1:0.4:596:72:2993. (Kazuyuki et al., 201).

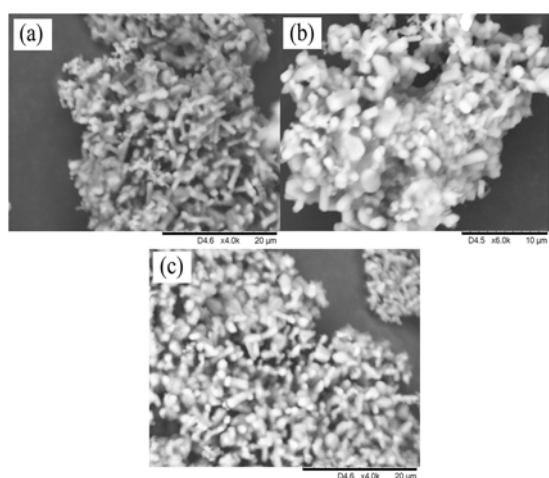


Figure 1. SEM images of MCM (a) MCM_Co(8hq)_2 (b) and $\text{MCMCo(II)}_8\text{hq}$ (c)

2.2.2 Synthesis mesoporous silica (MCM)

The ligand cobalt complex-mesoporous silica hybrids were obtained by solid-state reaction at room temperature (Pimchan et al., 2014). The amount of Co(II) cation determined by atomic absorption spectrometry (AAS) was 0.0332 mg/g. The hybrids were obtained by two different processes as follows; the first method 0.1 g of mesoporous silica (MCM), 0.0305 g of $\text{CoCl}_2 \cdot 6\text{H}_2\text{O}$, and 0.0648 g of 8hq at the molar ratio of 1:2 for Co(II) to 8hq ligand were mixed ground in a agate mortar at room temperature for 10-15 min (MCM_Co(8hq)_2) and the another method was ground step by step, 0.1 g of mesoporous silica with 0.0305 g of $\text{CoCl}_2 \cdot 6\text{H}_2\text{O}$ were mixed ground in a agate mortar at room temperature for 10-15 min then add 0.0648 g of 8hq (the molar ratio 1:2 for Co(II):8hq ligand) mixed ground in a agate mortar at room temperature for 10-15 min respectively ($\text{MCMCo(II)}_8\text{hq}$).

2.3 Characterization

Material characterizations: A HITACHI TM 3000 scanning electron microscope (SEM) was used for the identification of morphology and size of nanoparticles. X-ray Powder Diffraction patterns (XRD) were obtained on a Bruker D8 ADVANCE diffractometer using monochromic $\text{Cu K}\alpha$ radiation and Fourier-transform infrared spectroscopy (FTIR) was measured on a Spectrum One spectrometer over the spectral region of $600\text{--}4000\text{ cm}^{-1}$ by Bruker TENSOR27 confirmed the structural properties. The amount of metal ions were confirmed by atomic absorption spectrometry (AAS) on PinAAcle 900F Atomic absorption spectrometer. The result of optical properties by photoluminescence spectra were carried out from Spectrofluorometer FluoroMax 4 at the condition of a working voltage of 400 V and a slit width of 0.5 nm by the excitation of Xenon lamp at 320 nm.

3. Results and discussion

3.1 Mesoporous silica

The mesoporous silica was confirming the phase purity and identification through the SEM (Fig.1) and FT-IR (Fig.2). From the image (Fig.1) illustrated that the prominent morphology of particles is a mostly short rod-like cylinder and homogeneous aggregation of the particles is also observed. The diameters of particles approximately 1 µm and length up approximately 4 µm which is typically the morphology for mesoporous materials (Puratane & Amnuaypanich, 2018; Barczak, 2018; Cong, et al., 201). Figure 2. present the XRD patterns of mesoporous silica that the intensity of diffraction peaks at 2θ angles of 17.09° , 23.79° , 29.70° , 35.10° , 37.50° , 48.36° and 52.28° (JCPDS No. 16-0818), indicating that the crystalline phase of Na_2SiO_3 was the hexagonal phase (Li et al., 2019). The resulted of FT-IR spectrums demonstrate organic functional incorporation in silica framework (Fig.3) that the broad absorption band of 710 and 876 cm^{-1} corresponding Si-O-Si asymmetric bending and stretching respectively (Roschat et al., 2016), which were occurred from tetrahedral SiO_4 combination. The band due to 966 cm^{-1} shown stretching vibrations Si-OH (Yang et al., 2009; Yang et al., 2007; La-Salvia et al., 2017; Ogata, 2014). In addition, the absorption bands at 1428 cm^{-1} also corresponding Si=O formation (Roschat et, al. 2016) that the mesoporous silica morphology was confirmed.

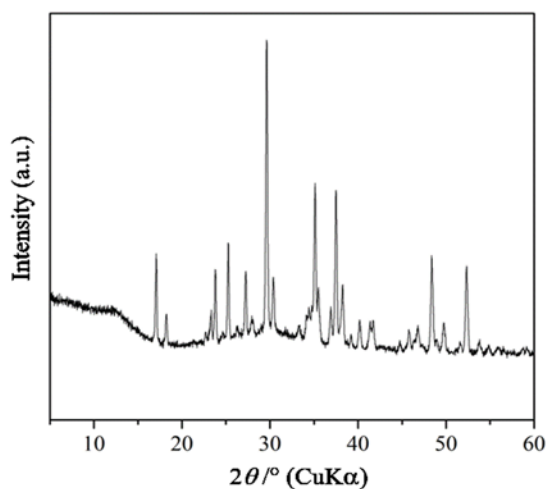


Figure 2. X-ray diffraction pattern of mesoporous silica from rice husk.

3.2 Bis(8-hydroxyquinoline)cobalt(II) into mesoporous silica

The preparation of the hybrid material of the cobalt (II) complex into mesoporous silica from the rice husk was confirmed by SEM, FT-IR and PL spectroscopies. Figure 1b. and 1c. showed the morphology after loading cobalt(II) complex into mesoporous silica from two different routes that the step by step ground product was obtained (Fig.1b) illustrated the microstructure was not changed from mesoporous silica (Fig. 1a). On the other hand, the hybrid material from mix ground method (Fig. 1c) was observed the little substances stuck on. The vibrations of CH₂ stretching as well as C-H vibration modes owing to the 8hq characteristics in Co(8hq)₂ and the FT-IR spectra of products are summarized in Figure 3. The absorption bands due to the C-H out of plane bending modes of the neat 8hq were observed at 815, 778, and 739 cm⁻¹, that all of the FT-IR spectra of the hybrids were shifted to higher frequencies were 820, 784 and 747 cm⁻¹ for MCM_Co(8hq)₂ as well as the frequencies of MCMCo(II)_8hq at 820, 786 and 747 cm⁻¹, confirming the coordination between cobalt (II) cation and 8-hydroxyquinoline (Pimchan et al., 2014). The stretching vibrations of metal oxide for tetrahedrally coordinated Co(II) ions of both products were observed at 645 and 647 cm⁻¹ respectively, indicating the formation of Co-O bonding in hybrid material (Li & Li, 2009; Saurav et al., 2015), supporting the interaction between hydroxyl group and cobalt(II) cation. A broad infrared absorption band in the region from 3000 to 3400 cm⁻¹ identified the water of hydration in the

samples (Li & Li, 2009), which was consistent with the photoluminescence spectra.

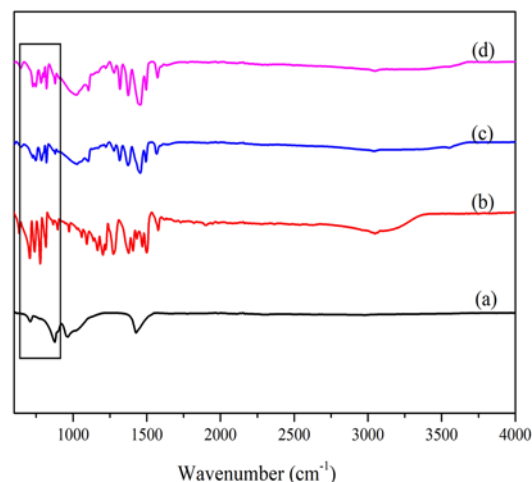


Figure 3. The FT-IR spectra of MCM (a), 8hq (b), MCM_Co(8hq)₂ (c) and MCMCo(II)_8hq (d)

Photoluminescence was a very important characteristic for the optical hybrid materials. All summaries were shown in Table 1. The luminescence spectrum of Co(8hq)₂ complex showed the emission band due to a π to π^* charge transfer from the electron-rich phenoxide ring to the electron-deficient pyridyl ring of the ligand at 468 nm (Li & Li, 2009). When the product from a mixed ground method, the luminescence maxima was observed at 484 nm for MCM_Co(8hq)₂, as well as the color appearance was a dark green-orange (Fig.5b). In another route, the intense emission band of MCMCo(II)_8hq hybrids revealed at 474 nm and the feature observe as light-green (Fig.5c). The maxima luminescence spectra of MCMCo(II)_8hq (474 nm) was blue-shifted, while MCM_Co(8hq)₂ was demonstrated identical the maxima luminescence spectra as cobalt(II) complex (484 nm) in this comparison reflected the change in HOMO/LUMO level and/or bandgap energy of the interaction complexes (Pimchan et al., 2014), implying that the cobalt complex with different nanostructures or packing formed either of cobalt(II) complexes in the mesoporous silica spaces. For example, the photoluminescence of cobalt(II)-bis(8-hydroxyquinoline) nanosheets were red-shifted and the fluorescence quenching when the cobalt(II)complex formation between p-nitroaniline molecules (Li & Li, 2009). The emission peak of CA[n]@SiO₂@CdTe nanoparticles (NPs) was red-shifted in comparison with its precursor SiO₂@CdTe nanoparticles, which may be attributed to the increased size of nanoparticles (Li & Qu, 2007), while zinc(II)-bis(8-hydroxyquinoline)

complex in channels of mesoporous silica nanoparticles (MSN) which functionalized with or without mercapto groups, the PL emission peaks of these samples are red-shifted from 500 nm for MSN-Zn(8hq) to 511 nm for MSN-SH₂-Zn(8hq), the optical properties of these samples are dependent on the interior circumstances and the concentration of mercapto groups in channels of MSNs (Li et al., 2012). In addition, the reported that the emission peak maxima of nanoporous silica-Al(8hq)₃, nanoporous silica-Al(8hq)₂ and Al(8hq)₃ are 505, 497, and 510 nm respectively. The greater blue-shift was observed in the emission spectra of nanoporous silica-Al(8hq)₂ can be attributed to changing the coordination sphere of Al ions in nanoporous silica-Al(8hq)₂ in comparison with nanoporous silica-Al(8hq)₃ (Badieli & Goldooz, 2012). From these observations, the formation of cobalt complex into mesoporous silica were proved.

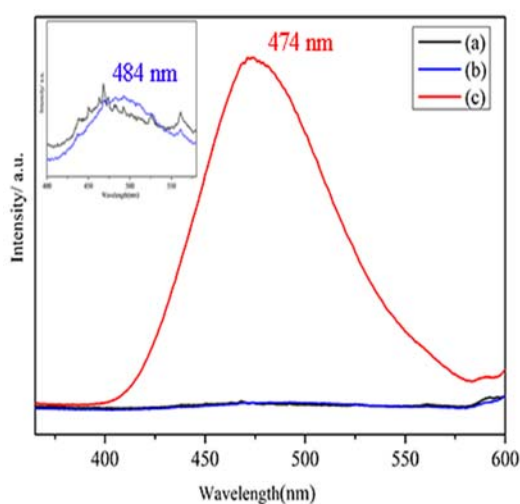


Figure 4. Luminescence spectra of Co(8hq)₂ (a), MCM_Co(8hq)₂ (b) and MCMCo(II)_8hq (c)



Figure 5. Colors of Co(8hq)₂ (a), MCM_Co(8hq)₂ (b) and MCMCo(II)_8hq (c)

In comparison of the luminescence efficiencies between MCM_Co(8hq)₂ and MCMCo(II)_8hq in Figure 4 demonstrates the excellence luminescence intensity of the hybrid material from step by step method (MCMCo(II)_8hq), while the other route

product (MCM_Co(8hq)₂) modulate insignificantly from Co(8hq)₂ complex, indicating the sequenced ground direction be able to efficiently improve the luminescence intensity of metal complex (Pimchan et al., 2014). It was illustrated that the cobalt(II) complex of 8-hydroxyquinoline was successfully prepared into mesoporous silica via solid-state reaction at room temperature and the immobilized complexes into mesoporous silica exhibited excellent photoluminescence properties. Moreover, the method via step by step ground affected the molecular structure and/or packing of the complexes, which are thought to be correlated with the increased luminescence efficiencies. From these observations, the hybrids material showed the outstanding photoluminescence efficiencies as well as the shift of luminescence maxima due to the energy level changes (Pimchan et al., 2014).

Finally, the instant system is preparation of mesoporous silica, which conventional method and advantage rice husk. Applications such as the host material, absorbent, and insulator as well as the cobalt(II) complexes complement ruled by the mesoporous silica host. Suggestions for the incorporation of the other ligand metal complexes with different metal ions, ligands and/or other host structures are foreshadowing because of the ease of operation, the enhancement of luminescence efficiencies and the stability of the incorporated complexes.

4. Conclusions

The mesoporous silica which was synthesized by swelling-shrinking mechanism from rice husk was successfully prepared. The preparation of hybrid materials via solid-state reaction between mesoporous silica and cobalt(II) ion, as well as 8-hydroxyquinoline at the room temperature. The emission maxima was 484 nm for MCM_Co(8hq)₂ hybrid and 474 nm of MCMCo(II)_8hq hybrid. The photoluminescence efficiency of MCMCo(II)_8hq hybrid was higher than MCM_Co(8hq)₂, indicating that the MCMCo(II)_8hq hybrid constitute an excellent optical properties material. The difference in microstructure and/or packing of the cobalt(II) complex into mesoporous silica could be adjusted by a variant of loading/packing method. The solid-state reaction is applicable to prepare various complexes in the porous hosts.

5. Acknowledgment

Department of Chemistry, Faculty of Science and Technology and Science center, Rajabhat Maha Sarakham University for the facilities provided. Our also extends to gratitude Promotion of Science and Mathematics Talented Teachers (PSMT) for partial financial support.

References

- Badiei, A., & Goldooz, H. (2012). A Simple Method for Preparation of Fluorescent Nanostructure Silica with Hexagonal Array. *International Journal of Modern Physics: Conference Series*, 05, 151-159. doi: 10.1142/S2010194512001961
- Badiei, A., Goldooz, H., Ziarani, G. M., & Abbasi, A. (2011). One pot synthesis of functionalized SBA-15 by using an 8-hydroxyquinoline-5-sulfonamide-modified organosilane as precursor. *Journal of Colloid and Interface Science*, 357(1), 63-69. doi:10.1016/j.jcis.2011.01.049
- Bakar, R. A., Yahya, R., & Gan, S. N. (2016). Production of High Purity Amorphous Silica from Rice Husk. *Procedia Chemistry*, 19, 189-195. doi:10.1016/j.proche.2016.03.092
- Barczak, M. (2018). Functionalization of mesoporous silica surface with carboxylic groups by Meldrum's acid and its application for sorption of proteins. *Journal of Porous Materials*, 26(1), 291-300. doi:10.1007/s10934-018-0655-7
- Behzad, S. K., Najafi, E., Amini, M. M., Janghour, M., Mohajerani, E., & Ng, S. W. (2014). Yellow-green electroluminescence of samarium complexes of 8-hydroxyquinoline. *Journal of Luminescence*, 156, 219-228. doi:10.1016/j.jlumin.2014.08.013
- Cong, V. T., Gaus, K., Tilley, R. D., & Gooding, J. J. (2018). Rod-shaped mesoporous silica nanoparticles for nanomedicine: recent progress and perspectives. *Expert Opinion on Drug*, 15(9), 881-892. doi:10.1080/17425247.2018.1517748
- He, X., Yu, C., Lin, J., Zhang, X., Li, Q., Fang, Y., ... Tang, C. (2018). Porous boron nitride/rare earth complex hybrids with multicolor tunable photoluminescence. *Journal of Alloys and Compounds*, 768, 15-21. doi:10.1016/j.jallcom.2018.07.160
- Jabariyan, S., & Zanjanchi, M. A. (2012). A simple and fast sonication procedure to remove surfactant templates from mesoporous MCM-41. *Ultrasonics Sonochemistry*, 19(5), 1087-1093. doi:10.1016/j.ultsonch.2012.01.012
- Kudo, T., Ito, T., & Kim, S.-Y. (2017). Adsorption Behavior of Sr(II) from High-level Liquid Waste using Crown Ether with Ionic Liquid Impregnated Silica Adsorbent. *Energy Procedia*, 131, 189-194. doi:10.1016/j.egypro.2017.09.426
- La-Salvia, N., Lovón-Quintana, J. J., Lovón, A. S. P., & Valença, G. P. (2017). Influence of Aluminum Addition in the Framework of MCM-41 Mesoporous Molecular Sieve Synthesized by Non-Hydrothermal Method in an Alkali-Free System. *Materials Research*, 20(6), 1461-1469. doi:10.1590/1980-5373-mr-2016-1064
- Li, B., Li, H., Zhang, X., Fan, P., Liu, L., Li, B., ... Zhao, B. (2018). Calcined sodium silicate as an efficient and benign heterogeneous catalyst for the transesterification of natural lecithin to L- α -glycerophosphocholine. *Green Processing and Synthesis*, 8, 78-84. doi:10.1515/gps-2017-0190
- Li, F., Li, H., & Cui, T. (2017). One-step synthesis of solid state luminescent carbon-based silica nanohybrids for imaging of latent fingerprints. *Optical Materials*, 73, 459-465. doi:10.1016/j.optmat.2017.09.004
- Li, H., & Li, Y. (2009). Synthesis of highly luminescent cobalt(II)-bis(8-hydroxyquinoline)nanosheets as isomeric aromatic amine probes. *Nanoscale*, 1(1), 128-132. doi:10.1039/B9NR00019D
- Li, H., & Qu, F. (2007). Selective inclusion of polycyclic aromatic hydrocarbons (PAHs) on calixarene coated silica nanospheres englobed with CdTe nanocrystals. *Journal of Materials Chemistry*, 17(33), 3536-3544. Doi: 10.1039/b705743a
- Li, H., Fu, Y., Zhang, L., Liu, X., Qu, Y., Xu, S., & Lü, C. (2012). In situ route to novel fluorescent mesoporous silica nanoparticles with 8-hydroxyquinolate zinc complexes and their biomedical applications. *Microporous and Mesoporous Materials*, 151, 293-302. doi:10.1016/j.micromeso.2011.10.021

- Li, K.-M., Jiang, J.-G., Tian, S.-C., Chen, X.-J., & Yan, F. (2014). Influence of Silica Types on Synthesis and Performance of Amine-Silica Hybrid Materials Used for CO₂ Capture. *Physical Chemistry C*, *118*(5), 2454-2462. doi:10.1021/jp408354r
- Liu, Y., Wang, Z., Zeng, H., Chen, C., Liu, J., Sun, L., & Wang, W. (2015). Photoluminescent mesoporous carbon-doped silica from rice husks. *Materials Letters*, *142*, 280-282. doi:10.1016/j.matlet.2014.12.034
- Ma, J. S., Lin, L. Y., & Chen Y. S. (2019). Facile solid-state synthesis for producing molybdenum and tungsten co-doped monoclinic BiVO₄ as the photocatalyst for photoelectrochemical water oxidation. *International Journal of Hydrogen Energy*, *44*(16), 7905-7914. doi:10.1016/j.ijhydene.2019.02.077
- Maučec, D., Šuligoj, A., Ristić, A., Dražić, G., Pintar, A., & Tušar, N. N. (2018). Titania versus zinc oxide nanoparticles on mesoporous silica supports as photocatalysts for removal of dyes from wastewater at neutral pH. *Catalysis Today*, *310*, 32-41. doi:10.1016/j.cattod.2017.05.061
- Nakamura, K. J., Ide, Y., & Ogawa, M. (2011). Molecular recognitive photocatalytic decomposition on mesoporous silica coated TiO₂ particle. *Materials Letters*, *65*(1), 24-26. doi:10.1016/j.matlet.2010.09.043
- Ogata Y.H. (2018) *Characterization of Porous Silicon by Infrared Spectroscopy*. In: Canham L. (eds) Handbook of Porous Silicon. Springer, Cham.
- Patel, V. K., Saurav, J. R., Gangopadhyay, K., Gangopadhyay, S., & Bhattacharya, S. (2015). Combustion characterization and modeling of novel nanoenergetic composites of Co₃O₄/nAl. *RSC Advances*, *5*(28), 21471-21479. doi: 10.1039/c4ra14751k
- Patriarca, M., Daier, V., Camí, G., Pellegrini, N., Rivière, E., Hureau, C., & Signorella, S. (2019). Biomimetic Cu, Zn and Cu₂ complexes inserted in mesoporous silica as catalysts for superoxide dismutation. *Microporous and Mesoporous Materials*, *279*, 133-141. doi:10.1016/j.micromeso.2018.12.027
- Pimchan, P., Khaorapapong, N., Sohmiya, M., & Ogawa, M. (2014). In situ complexation of 8-hydroxyquinoline and 4,4'-bipyridine with zinc(II) in the interlayer space of montmorillonite. *Applied Clay Science*, *95*, 310-316. doi:10.1016/j.clay.2014.04.033
- Pimprom, S., Sriboonkham, K., Dittanet, P., Föttinger, K., Rupprechter, G., & Kongkachuichay, P. (2015). Synthesis of copper-nickel/SBA-15 from rice husk ash catalyst for dimethyl carbonate production from methanol and carbon dioxide. *Journal of Industrial and Engineering Chemistry*, *31*, 156-166. doi:10.1016/j.jiec.2015.06.019
- Puratane, C. & Amnuaypanich, S. (2018). Mesoporous silica particles (MSPs) prepared by diol-functionalized natural rubber (ENR50-diol) and cationic surfactant (CTAB) dual templates, *KKU Sci. J.* *46*(3), 496-505.
- Rahman, A. Z. M. S. (2016). *Solid State Luminescent Materials: Applications. Reference Module in Materials Science and Materials Engineering*. doi:10.1016/b978-0-12-803581-8.04078-9
- Roschat, W., Siritanon, T., Yoosuk, B., & Promarak, V. (2016). Rice husk-derived sodium silicate as a highly efficient and low-cost basic heterogeneous catalyst for biodiesel production. *Energy Conversion and Management*, *119*, 453-462. doi:10.1016/j.enconman.2016.04.071
- Sábio, R. M., Gressier, M., Caiut, J. M. A., Menu, M.-J., & Ribeiro, S. J. L. (2016). Luminescent multifunctional hybrids obtained by grafting of ruthenium complexes on mesoporous silica. *Materials Letters*, *174*, 1-5. doi:10.1016/j.matlet.2016.03.058
- Singh, D., Nishal, V., Bhagwan, S., Saini, R. K., & Singh, I. (2018). Electroluminescent materials: Metal complexes of 8-hydroxyquinoline-A review. *Materials & Design*, *156*, 215-228. doi:10.1016/j.matdes.2018.06.036
- Sohmiya, M., & Ogawa, M. (2011). Controlled spatial distribution of tris(2,2'-bipyridine)ruthenium cation ([Ru(bpy)₃]²⁺) in aluminum containing mesoporous silicas. *Microporous and Mesoporous Materials*, *142*(1), 363-370. doi:10.1016/j.micromeso.2010.12.023

- Sohmiya, M., Saito, K., & Ogawa, M. (2015). Host-guest chemistry of mesoporous silicas: precise design of location, density and orientation of molecular guests in mesopores. *Science and Technology of Advanced Materials*, 16(5), 1-17. doi:10.1088/1468-6996/16/5/054201
- Świdorski, G., Kalinowska, M., Wilczewska, A. Z., Malejko, J., & Lewandowski, W. (2018). Lanthanide complexes with pyridinecarboxylic acids-Spectroscopic and thermal studies. *Polyhedron*, 150, 97-109. doi:10.1016/j.poly.2018.04.045
- Tsuboi, T., Nakai, Y., & Torii, Y. (2012). Photoluminescence of bis(8-hydroxyquinoline) zinc (Znq_2) and magnesium (Mgq_2). *Open Physics*, 10(2). doi:10.2478/s11534-011-0090-8
- Vibulyaseak, K., Deepracha, S., & Ogawa, M. (2018). Immobilization of titanium dioxide in mesoporous silicas; structural design and characterization. *Solid State Chemistry*, 270, 162-172. doi:10.1016/j.jssc.2018.09.043
- Yang, J., Chen, J., & Song, J. (2009). Studies of the surface wettability and hydrothermal stability of methyl-modified silica films by FT-IR and Raman spectra. *Vibrational Spectroscopy*, 50(2), 178-184. doi:10.1016/j.vibspec.2008.09.016
- Yang, P., Quan, Z., Lu, L., Huang, S., Lin, J., & Fu, H. (2007). MCM-41 functionalized with $YVO_4:Eu^{3+}$: a novel drug delivery system. *Nanotechnology*, 18(23), 1-10. doi:10.1088/0957-4484/18/23/235703
- Zhang, X., Tang, J., Li, H., Wang, Y., Wang, X., Wang, Y., Huang, L., & Belfiore, L. A. (2018). Red light emitting nano-PVP fibers that hybrid with $Ag@SiO_2@Eu(tta)_3phen$ -NPs by electrostatic spinning method. *Optical Materials*, 78, 220-225. doi:10.1016/j.optmat.2018.02.014
- Zhao, H., Zhang, T., Qi, R., Dai, J., Liu, S., Fei, T., & Lu, G. (2017). Organic-inorganic hybrid materials based on mesoporous silica derivatives for humidity sensing. *Sensors and Actuators B: Chemical*, 248, 803-811. doi:10.1016/j.snb.2016.11.104